# A Variable Temperature Walters Spiral Probe for the Critical Current Measurement of Superconducting Strands

Sangjun Oh, Chulhee Lee, Heekyung Choi, Kyungmo Moon, Keeman Kim, Jiman Kim, and Pyeong-Yeol Park

***Abstract*—We have developed a probe for the critical current measurements of low temperature superconducting strands at various field, temperature and strain. A 30 cm-long strand sample is soldered on a Walters spiral made of beryllium copper alloy and compressive or tensile axial strain can be applied up to 0.7%. Temperature control ability was tested using a $MgB_2$ wire up to 30 K. Three cernox sensors are attached on a spiral adjacent to the strand and the temperature of the spiral is controlled within $\pm$50 mK of target temperature during the critical current measurement up to 80 A. Extensive critical current measurements have been carried out for an internal-tin processed $Nb_3Sn$ strand. It was found that the measured field, temperature and strain dependence of the critical current for the internal-tin $Nb_3Sn$ strand is in agreement with the recent scaling law based on strong coupling theory of superconductivity.**

***Index Terms*—Eliashberg theory, scaling law for flux pinning, strain dependence of the critical current, Walters spiral probe.**

## I. Introduction

EVER since the early report of Ekin [1], where detailed measurement results for the strain dependence of the critical current of various $Nb_3Sn$ strands using an apparatus employing axial pulling method on a hanging strand sample were reported, various probes have been developed. A notable improvement had been made by Walters *et al.* [2], who used a thick spiral spring, now usually called Walters spiral, as a strain transmitting medium. A strand sample is soldered on the periphery of the spiral and the external axial strain is applied to the sample by twisting the spiral. Since the sample is firmly soldered on the spiral, no additional support against the Lorentz force is needed and both compressive and tensile axial strain can be applied. The method of using a thick solid beam curved or straight for the application of strain with a sample soldered around it is adapted for other probes as well such as the U-shape probe reported by ten Haken *et al.* [3], the so-called Pacman probe reported by Godeke *et al.* [4] or the horseshoe type probe recently developed by Nunoya *et al.* [5].

Another merit of Walters spiral is that it can accommodate long sample and as a result more stable voltage measurements become possible. We have developed our own Walters spiral probe which can measure the critical current for a 30 cm-long sample and a comparative study using the Walters spiral probe on 4.2 K strain dependence of the critical current for various internal-tin processed $Nb_3Sn$ strands has been reported [6]. The probe is further improved for the critical current measurement at various temperatures. Detailed temperature control methods and test results up to 30 K using a $MgB_2$ wire sample are presented in Section II. Using the variable temperature Walters spiral probe, extensive field, temperature and strain dependence of the critical current for an internal-tin processed $Nb_3Sn$ strand has been measured and is compared with the recent scaling law based on strong coupling theory of superconductivity in Section III.

Manuscript received August 29, 2007. This work was supported by the Korea Ministry of Science and Technology of Republic of Korea under the ITER Project Contract.

S. Oh, C. Lee, H. Choi, K. Moon, and K. Kim are with the National Fusion Research Center, Daejeon, 305-333 Korea (e-mail: wangpi@nfrc.re.kr).

J. Kim and P.-Y. Park are with KAT (e-mail: pypark@kiswire.com).

Color versions of one or more of the figures in this paper are available online at http://ieeexplore.ieee.org.

Digital Object Identifier 10.1109/TASC.2008.921254

## II. Development of a Variable-Temperature Walters Spiral Probe

A schematic cross-sectional view for the bottom part of the developed variable temperature Walters spiral probe is presented in Fig. 1. As noted in our previous work [6], the way to apply a torque on the spiral is quite similar to that reported by Cheggour and Hampshire [7]. A 4.5 turn Walters spiral made of BeCu alloy is tightly mounted between glass fiber reinforced plastic (GFRP) holders with in-between stainless steel pins. Whereas the bottom holder firmly fastened to the outer stainless steel tube is fixed, the top holder attached to the inner thick tube rotates. The top end of the inner stainless steel tube is connected with a worm-wheel gear and there is an indicator for the rotation angle between the inner and outer tube. The primary role of the GFRP holders is electrical insulation but the bottom GFRP holder also works as a supporting structure. For the critical current measurements at various temperatures, the sample space is vacuum sealed and especially the bottom part of the probe is indium sealed. Oxygen-free high-conductivity (OFHC) copper current leads are also indium sealed using fixtures made of GFRP. A 30 cm long strand sample is soldered on the periphery of the spiral as shown in the inset of Fig. 1. The distance between voltage tabs is 15 cm and both compressive and tensile axial strain can be applied up to 0.7%. Details of sample preparation and the procedure of the critical current measurement are described in our previous report [6]. After the current leads are soldered on the both end of the spiral, three Cernox sensors are attached on the surface of the upper, middle and lower part of the spiral adjacent to the strand sample using Stycast epoxy.

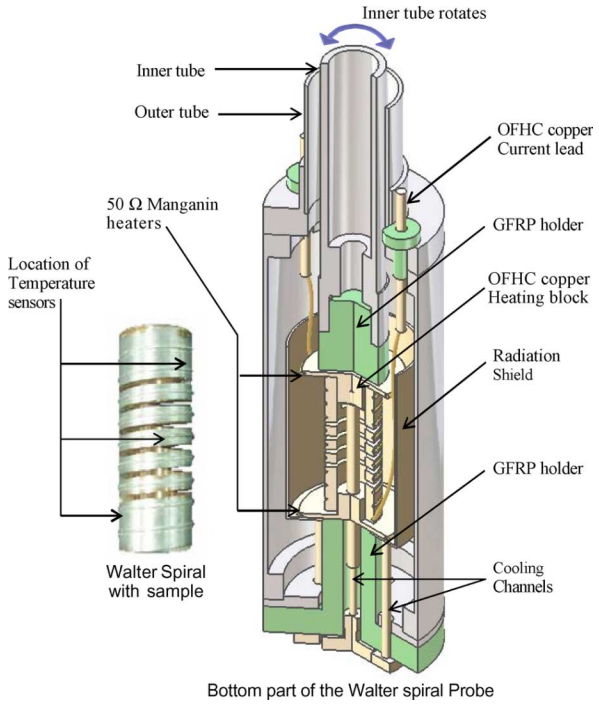


Fig. 1. A schematic cross-sectional view for the bottom part of the variable temperature Walters spiral probe. *Inset*: A photograph of the Walters spiral with a sample soldered around it.

The temperatures of the upper and lower parts of the spiral are actively controlled by OFHC copper blocks inserted in between the spiral and the GFRP holders. Heating power is supplied by 50 Ω Manganin wires wound around the outer circumference of the copper blocks and is controlled by Lakeshore 340 temperature controllers. Two copper blocks are connected with OFHC copper rods which act as cooling channels. The bottom ends of the copper rods are facing liquid helium directly. The copper rod connected with the upper copper block goes through the spiral and is wrapped around by about 5 layers of aluminized Mylar superinsulation to reduce radiation. Since the upper copper block rotates together as the spiral is twisted, the copper rod is separated into two pieces and thermally linked by a bunch of flexible copper wires. To cut radiation and to increase temperature uniformity, the spiral is covered with a OFHC copper tube which is thermally anchored to the temperature-controlled lower copper block. After the temperatures of the upper and lower parts of the spiral settle down to target temperature, about 0.1 torr of helium exchange gas is inserted into the sample space. Without exchange gas, the temperature of the middle part gradually increases over the target temperature and saturates at about 18 K, for example, if the target temperature is set to 15 K. As we increase the amount of exchange gas, the temperature of the middle part of the spiral is lowered and is finally stabilized to the target temperature. The pressure of the exchange gas is monitored on top of the probe and is varied with environmental change such as the helium level of the cryostat. Prior to the critical current measurements, the field dependence of the temperature sensors was calibrated.

Temperature control ability during the critical current measurement was tested up to 30 K using a multi-filamentary Hyper Tech $MgB_2$ strand. The $MgB_2$ strand was heat treated at 650 °C

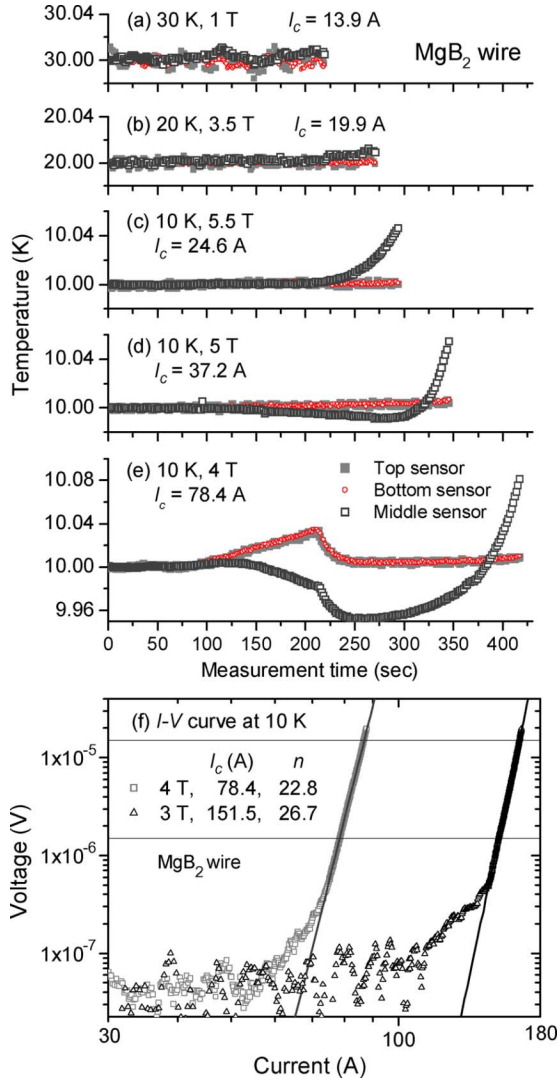


Fig. 2. Temperature fluctuation during the critical current measurement. (f): measured $I-V$ characteristics for the Hyper Tech $MgB_2$ wire.

for 30 minutes. Temperature variations during the critical current measurements are shown in Fig. 2. The current ramp rate was about 0.24 A/sec if the observed voltage signal was less than 0.7 $\mu$V and was about 0.06 A/sec above 0.7 $\mu$V. For the critical current less than 20 A, the temperatures of the upper, middle and lower part of the spiral are controlled within $\pm 10$ mK during the critical current measurements as can be seen in Fig. 2(a) and (b), whereas for the critical current above 20 A, the temperature of the middle part increased up to 50 mK above the target temperature at the end of current ramp-up [Fig. 2(c)]. If the applied current is larger than 30 A, we observe that the temperature of the middle part gradually decreases below the target temperature as the applied current is increased as can be seen in Fig. 2(d). It seems to be related with the sample space local pressure increase by the heating power from the current leads. This behavior can be more clearly seen in Fig. 2(e). At a faster ramp rate, even the temperatures of the upper and lower part gradually increase due to the heating power from the leads if the applied current is larger than about 40 A. Once the ramp rate is slowed down, the temperatures of the upper and lower part are settled down to the target temperature while the temperature of the

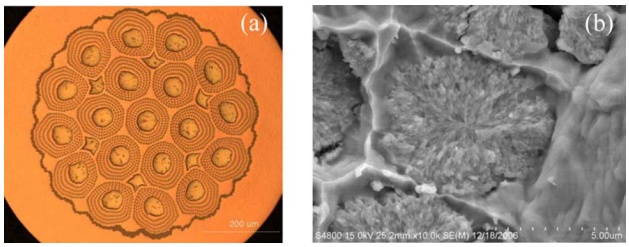


Fig. 3. Optical microscope and FE-SEM images before and after heat treatment for a KAT internal-tin processed $Nb_3Sn$ strand.

middle part is about 50 mK below the target temperature. The current-voltage characteristic curve corresponding to Fig. 2(e), measured at 10 K and 4 T, is shown in Fig. 2(f). The critical current is defined at an electric field criterion of 0.1 $\mu$V/cm and the $n$-value is obtained from the fitting within the electric field range of 0.1–1 $\mu$V/cm. Even the critical current up to ~150 A can be measured as can be seen in Fig. 2(f) but the temperature variation of the middle part was more than 150 mK.

## III. Field, Temperature and Strain Dependences of the Critical Current for an Internal-Tin $Nb_3Sn$ Strand

Detailed critical current measurements have been made for an internal-tin processed $Nb_3Sn$ strand. The field, temperature and strain dependence of the critical current for $Nb_3Sn$ strands have been studied a lot and can be compared with recent scaling law for flux pinning [8]–[10]. An internal-tin strand manufactured by KAT (Kiswire Advanced Technology) was heat treated at 210 °C for 50 hours, 340 °C for 25 hours, 450 °C for 25 hours, 575 °C for 100 hours and finally at 650 °C, 100 hours. The temperature is ramped up at a rate of 5°C/hour. An optical microscope image before the heat treatment and a FE-SEM (field emission scanning electron microscopy) image after the heat treatment are shown in Fig. 3.

The field and strain dependence of the critical current for the internal-tin processed $Nb_3Sn$ strand at 4.2, 10 and 14 K are shown in Fig. 4. The strain dependence of the critical current shows its maximum ($\varepsilon_{max}$) when the applied strain ($\varepsilon_{app}$) is +0.372%. All the data shown in Fig. 4 are presented as a function of an intrinsic strain ($\varepsilon_{int}$) defined as $\varepsilon_{int} = \varepsilon_{app} - \varepsilon_{max}$. Kramer plots for 10 and 14 K data are shown in Fig. 5. Near the upper critical field, positive curvatures in the Kramer plots were observed, which are usually attributed to either microstructural or compositional inhomogeneities [10]. We recently reported on a possibility of thermal activation for the origin of the positive curvatures in Kramer plots which was discussed in relation with the field dependence of the $n$-value [11]. In this work, however, only the data above about 5 $A^{0.5}$ $T^{0.25}$, from which the upper critical field and the pinning force maximum can be obtained by a linear extrapolation, were analyzed for simplicity.

The temperature and strain dependence of the extracted upper critical field $B^*_{c2}$ and the pinning force maximum $F_m$ shown in Figs. 6 and 7 are compared with a recent scaling law based on strong coupling theory of superconductivity [9]. The temperature and strain dependence of intrinsic superconducting parameters, such as the Ginzburg-Landau parameter and the upper critical field, were obtained from calculation results using Eliashberg theory [12] for representative model cases. It was shown

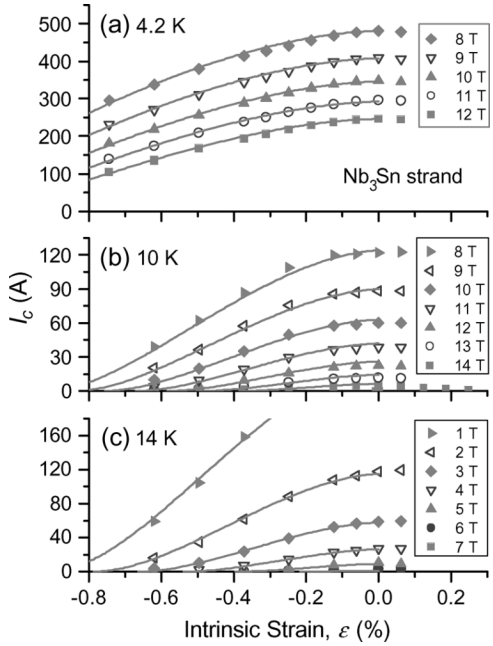


Fig. 4. The field, temperature and strain dependence of the critical current for the KAT internal-tin processed $Nb_3Sn$ strand.

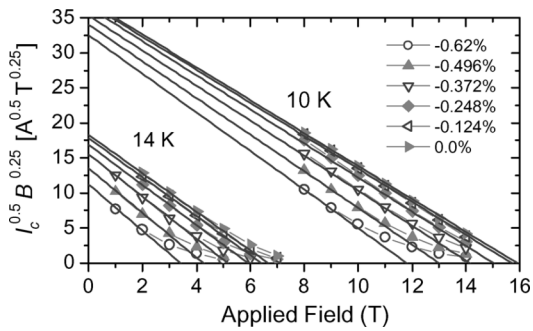


Fig. 5. Kramer plots for the KAT internal-tin $Nb_3Sn$ strand at 10 and 14 K.

that if the strain dependence of the critical temperature can be described by $T_c(\varepsilon) = T_c(0)(1 - \alpha|\varepsilon|^{1.7})$, then the thermodynamic critical field can be written as $B_c(T,\varepsilon) = B_c(0,0)(1 - \beta|\varepsilon|^{1.7})(1 - t^{2.17})$, with $t = T/T_c$. And the upper critical field $B_{c2}$ and the pinning force maximum $F_m$ can be expressed as [9],

$$\begin{aligned} B_{c2}(T,\varepsilon) &= B_{c2}(0,0)\left(1-\beta|\varepsilon|^{1.7}\right)\left(1-\gamma|\varepsilon|^{1.7}\right) \\ &\quad \times (1-t^{2.17})k(t,\varepsilon) \\ F_m(T,\varepsilon) &= F_m(0,0)\left(1-\beta|\varepsilon|^{1.7}\right)^{5/2}\left(1-\gamma|\varepsilon|^{1.7}\right)^{1/2} \\ &\quad \times (1-t^{2.17})^{5/2}k(t,\varepsilon)^{1/2} \end{aligned} \tag{1}$$

where,

$$k(t,\varepsilon) = \left(1 + u\frac{1-\gamma|\varepsilon|^{1.7}}{1-\alpha|\varepsilon|^{1.7}}(1-t^v)\right) \Big/ \left(1 + u\frac{1-\gamma|\varepsilon|^{1.7}}{1-\alpha|\varepsilon|^{1.7}}\right)$$

The strain dependence of the critical temperature $T_c$, the thermodynamic critical field $B_c$ and the Ginzburg-Landau parameter are described by coefficients $\alpha$, $\beta$ and $\gamma$, respectively, and

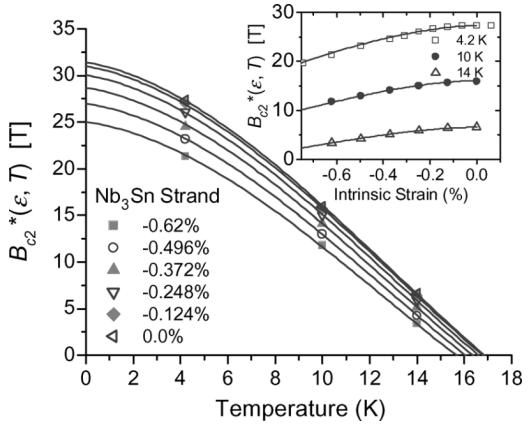


Fig. 6. The extrapolated upper critical field as a function of temperature and strain for the KAT internal-tin processed $Nb_3Sn$ strand.

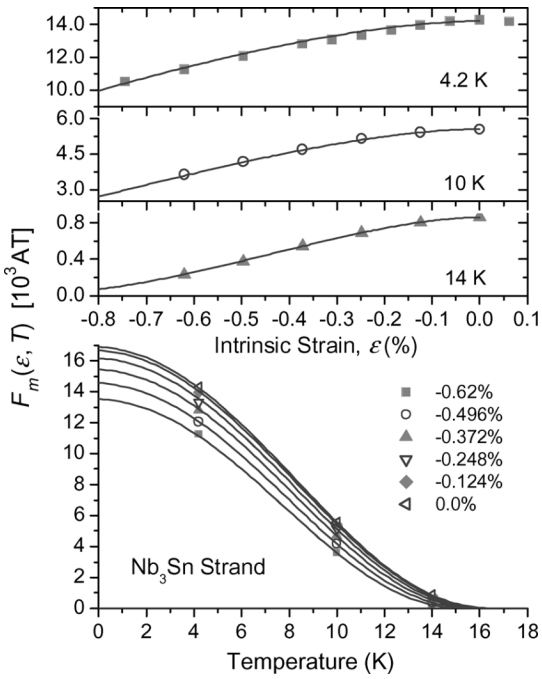


Fig. 7. The pinning force maximum as a function of temperature and strain for the KAT internal-tin processed $Nb_3Sn$ strand.

the parameters $u$ and $v$ are related with the temperature dependence of the Ginzburg-Landau parameter or the upper critical field $B_{c2}$. The temperature and strain dependence of the pinning force maximum $F_m$ is obtained following the Kramer flux line lattice shearing model,

$$I_c \times B = F_m(T,\varepsilon)\cdot b^{1/2}(1-b)^2 \propto B_{c2}^{5/2}\kappa^{-2}\cdot b^{1/2}(1-b)^2, \quad (2)$$

where, the reduced field $b$ is defined as a ratio between the applied field and the upper critical field, $b = B/B_{c2}$.

The fit parameters $\beta$ and $\gamma$ can be estimated from the 4.2 K strain dependence of $B_{c2}^*$ and $F_m$ [9], [11]. All other parameters except $F_m(0,0)$ were obtained from the fitting of the temperature and strain dependence of the upper critical field. All lines in Figs. 6 and 7 calculated with (1) using the parameters listed in Table I, are in agreement with the extrapolated data. Due to limited number of data in the tensile region, only the data in the compressive region were analyzed. The measured critical current data also can be calculated with (1) and (2) using the same parameters as can be seen in Fig. 4.

TABLE I
FITTING PARAMETERS FOR THE KAT INTERNAL-TIN $Nb_3Sn$ STRAND

| $\alpha$ | $\beta$ | $\gamma$ | $u$ | $v$ | $T_c(0)$ | $B_{c2}(0,0)$ | $F_m(0,0)$ |
|---|---|---|---|---|---|---|---|
| 400 | 300 | 900 | 0.85 | 1.2 | 16.87 K | 31.4 T | 16900 AT |

## IV. CONCLUSION

In Summary, we have successfully developed a Walters spiral probe for the critical current measurements of superconducting strands at various field, temperature and strain. Using the probe, detailed critical current measurements have been performed for an internal-tin processed $Nb_3Sn$ strand and the measured field, temperature and strain dependence of the critical current is in agreement with the recent scaling law based on strong coupling theory of superconductivity. Temperature control ability during the critical current measurement was tested up to 30 K and the developed probe can be further utilized for the characterization of other low temperature superconducting strands such as $MgB_2$ wires.

## REFERENCES

[1] J. W. Ekin, "Strain scaling law for flux pinning in practical superconductors. Part I: Basic relationship and application to $Nb_3Sn$ conductors," *Cryogenics*, vol. 20, pp. 611–624, Nov. 1980.

[2] C. R. Walters, I. M. Davidson, and G. E. Tuck, "Long sample high sensitivity critical current measurements under strain," *Cryogenics*, vol. 26, pp. 406–412, Jul. 1986.

[3] B. ten Haken, A. Godeke, and H. H. J. ten Kate, "The strain dependence of the critical properties of $Nb_3Sn$ conductors," *J. Appl. Phys.*, vol. 85, pp. 3247–3253, Mar. 1999.

[4] A. Godeke, M. Dhalle, A. Morelli, L. Stobbelaar, H. van Weeren, H. J. N. van Eck, W. Abbas, A. Nijhuis, A. den Ouden, and B. ten Haken, "A device to investigate the axial strain dependence of the critical current density in superconductors," *Rev. Sci. Instrum.*, vol. 75, no. 12, pp. 5112–5118, Dec. 2004.

[5] Y. Nunoya, T. Isono, N. Koizumi, K. Hamada, K. Matsui, Y. Nabara, and K. Okuno, "Development of strain-applying apparatus for evaluation of ITER $Nb_3Sn$ strand," *IEEE Trans. Appl. Supercond.*, vol. 17, pp. 2588–2590, Jun. 2007.

[6] S. Oh, S. H. Park, C. Lee, Y. Chang, K. Kim, and P.-Y. Park, "A strain dependence of critical current in internal Tin process $Nb_3Sn$ strands," *IEEE Trans. Appl. Supercond.*, vol. 15, pp. 3462–3465, Jun. 2005.

[7] N. Cheggour and D. Hampshire, "A probe for investigating the effects of temperature, strain, and magnetic field on transport critical currents in superconducting wires and tapes," *Rev. Sci. Instrum.*, vol. 71, no. 12, pp. 4521–4530, Dec. 2000.

[8] D. M. J. Taylor and D. P. Hampshire, "The scaling law for the strain dependence of the critical current density in $Nb_3Sn$ superconducting wires," *Supercond. Sci. Technol.*, vol. 18, pp. S241–S252, Nov. 2005.

[9] S. Oh and K. Kim, "A scaling law for the critical current of $Nb_3Sn$ stands based on strong-coupling theory of superconductivity," *J. Appl. Phys.*, vol. 99, p. 033909, Feb. 2006.

[10] A. Godeke, B. ten Haken, H. H. J. ten Kate, and D. C. Larbalestier, "A general scaling relation for the critical current density in $Nb_3Sn$," *Supercond. Sci. Technol.*, vol. 19, pp. R100–R116, Sep. 2006.

[11] S. Oh, C. Lee, K. W. Cho, K. Kim, D. Uglietti, and R. Flükiger, "Field dependence of the $n$-value and its relation with the critical current of $Nb_3Sn$ strands," *Supercond. Sci. Technol.*, vol. 20, pp. 851–858, Jul. 2007.

[12] M. Schossmann and E. Schachinger, "Strong-coupling theory of the upper critical magnetic field $H_{c2}$," *Phys. Rev. B*, vol. 33, pp. 6123–6131, May 1986.